FDG Hypermetabolism Associated with Inflammatory Necrotic Changes Following Radiation of Meningioma

Alan J. Fischman, Allan F. Thornton, Matthew P. Frosch, Brooke Swearinger, R.G. Gonzalez and Nathaniel M. Alpert
Departments of Radiology, Radiation Medicine, Pathology and Neurosurgery, Massachusetts General Hospital and Harvard Medical School, Boston Massachusetts

PET with ^{18}F-fluoro-2-deoxy-D-glucose (FDG) is currently the noninvasive gold standard for distinguishing brain tumor recurrence from radiation necrosis. We present a case report that appears to contradict this doctrine. The patient had a history of atypical meningioma and was treated with surgical resection and postoperative proton-beam radiation therapy. Approximately 16 mo after completion of therapy, MRI demonstrated two new regions of enhancement, and an FDG-PET study was performed to further characterize these lesions. FDG-PET demonstrated an area of intense hypermetabolism, and wide surgical resection was performed. Histological examination of the surgical specimen revealed reactive changes and areas of necrosis. There was no evidence of either recurrent or radiation-induced tumor.

Key Words: fluorine-18-FDG; PET; meningioma

J Nucl Med 1997; 38:1027–1029

Metabolic imaging with ^{18}F-fluoro-2-deoxy-D-glucose (^{18}F-FDG) for differentiating between recurrent high-grade tumor and radiation necrosis is among the most common clinical applications of PET in patients with primary brain tumors. The critical FDG-PET finding in these studies is focal hypometabolism in the areas of necrosis, in contrast with the hypermetabolism that is associated with residual/recurrent high-grade tumor. Currently, FDG-PET is the noninvasive gold standard for making this critical clinical decision (*1–3*) and is considerably more accurate than conventional CT (*4*) or MRI (*5*).

Since many astrocytoma brain tumor recurrences are of higher grade than the primary lesion, differentiation from necrosis is straightforward. However, with some low- or intermediate-grade lesions, recurrences can be of similar grade. Thus, if the primary tumor was eumetabolic relative to normal gray matter, new small enhancing MRI lesions that are adjacent to or in gray matter may be difficult to evaluate by FDG-PET. Under these circumstances, precise co-registration of PET images with anatomic imaging studies can be extremely helpful. Recently, a case of this type in which radiation necrosis was incorrectly diagnosed with FDG-PET was reported (*6*). When recurrence occurs in white matter or in a hypometabolic radiation field, tumor detection and differentiation from radiation necrosis is simplified.

These considerations limit the sensitivity of FDG-PET for differentiating small regions of low-grade tumor recurrence from radiation necrosis. However, when a region of MRI enhancement corresponds to an area of intense hypermetabolism of FDG, radiation necrosis can be excluded with an extremely high degree of certainty. In this article, we present a case report which appears to contradict this doctrine, i.e., intense FDG accumulation associated with reactive changes and radiation necrosis.

Received Aug. 1, 1996; revision accepted Oct. 30, 1996.
For correspondence or reprints contact: Alan J. Fischman, MD, Division of Nuclear Medicine, Massachusetts General Hospital, 32 Fruit St., Boston, MA 02114.

CASE REPORT

A 68-yr-old woman, who initially presented with several months of increasing fatigue, bifrontal headache, left-sided weakness and periods of confusion, was included in our study. A CT scan with contrast demonstrated a dural-based mass in the right sphenoid; approximately 3.5 cm in diameter with significant edema and 1.5-cm midline shift. The presence of tumor was confirmed by angiography; however, embolization was not considered to be feasible due to ophthalmic artery collaterals. A right frontotemporal craniotomy was performed, and approximately 60% of the tumor mass was resected. Due to proximity to critical structures, the tumor was not resected from the right cavernous sinus. Pathological examination of the surgical specimen revealed sheets of a tumor with occasional mitotic figures and foci of necrosis. The tumor cells had prominent nucleoli. Although the tumor was closely adherent to the brain in several regions, there was no clear evidence of brain invasion. The final diagnosis was atypical meningioma.

Five months after surgery, the residual tumor was treated with stereotactic proton-beam radiation. Because of the poor local control rates of atypical meningiomas with standard dose (50–55 Gy radiation used for benign meningioma), 68.4 Gy was delivered at ~1.8 Gy/day. MRI performed both before and 1 mo after therapy demonstrated residual focal nodular enhancement encasing the right supraclinoid ICA segment and mild residual right parasellar mass effect representing residual meningioma. In another MRI performed 4 mo later, the residual right parasellar mass effect was less prominent. Eighteen months after radiation therapy, the patient remained clinically stable; however, a routine follow-up MRI revealed two ~3 mm areas of enhancement, one in the right optic tract and one in the right choroidal fissure. These abnormalities were thought to represent either post-radiation necrosis or recurrent tumor. Since the patient's neurological examination remained stable, it was elected to closely follow the lesions by serial MR imaging. Six weeks later, MRI demonstrated that both lesions had increased in size, and an FDG-PET study was performed to further characterize the abnormalities.

PET images were acquired with a PC-4096 PET camera (Scanditronix AB, Uppsala, Sweden) (*7*). The primary imaging parameters of the camera were in-plane and axial resolutions of 6.0 mm FWHM, 15 contiguous slices of 6.5 mm separation and a sensitivity of ~135 cps/KBq. All images were reconstructed using a conventional filtered backprojection algorithm to an in-plane resolution of 7-mm FWHM. All projection data were corrected for nonuniformity of detector response, dead time, random coincidences and scattered radiation. Regions of interest (ROIs) were circular with a fixed diameter of 16 mm. An analytic attenuation correction was applied to the data based on an estimate of slice

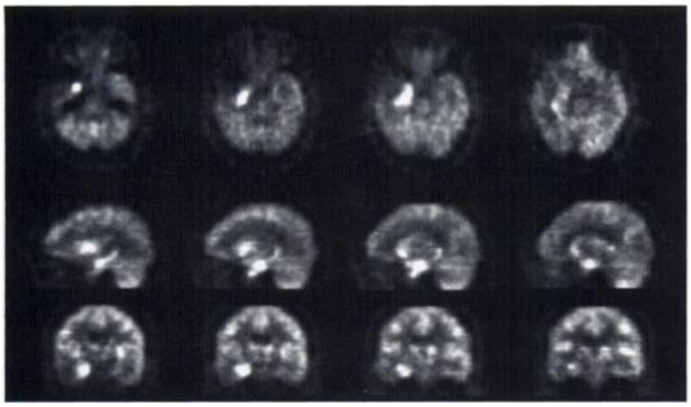

FIGURE 1. Representative transaxial (upper row), sagittal (middle row) and coronal (lower row) FDG-PET images.

contour and the assumption of a uniform attenuation coefficient equal to that of water.

Fluorine-18-FDG (370 MGq, 10 mCi) was injected intravenously, while the patient was in a quiet room with eyes open. After a 45-min uptake period, the subject's head was immobilized with a custom fabricated head-holder. There was no clinical evidence of seizure activity during the FDG uptake period. The imaging plane was parallel to the orbito-meatal line. Due to the limited field of view of the scanner, emission data were acquired in two bed positions; each scan was of 15 min duration. The PET data were co-registered with MR images using software developed in our laboratory (*8*), and the fusion images were evaluated visually. Semiquantitative analysis was performed by calculating lesion to contralateral gray and white matter ratios (L/G and L/W).

The FDG-PET images demonstrated an extensive area of hypermetabolism, extending from the right posterior parasellar region to the medial mid and anterior right temporal lobe (Fig. 1). The area of hypermetabolism was approximately 2–3 cm in length and 1.5 cm in width and corresponded with the MRI abnormality (Fig. 2).

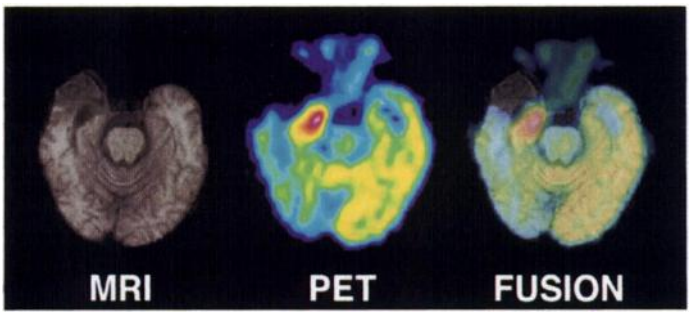

FIGURE 2. Co-registered FDG-PET and MR images at the plane of maximal FDG accumulation demonstrates concordance of the functional and anatomic abnormalities. The corresponding fusion image is also shown. PET images were acquired approximately 1 mo after MRI.

The maximal L/G and L/W ratios were 1.37 and 4.40, respectively. Accumulation of FDG in the remainder of the right temporal lobe and the right parietal lobe was mildly decreased, consistent with previous radiation therapy. Normal activation of the visual cortex was observed. There was no evidence of abnormal FDG accumulation in the remainder of the brain.

Due to the possibility of either treatable resectable recurrence or a second malignancy, surgical resection and decompression was performed. Postoperative MRI confirmed that the region of increased FDG accumulation was contained within the resected volume of tissue. Histological evaluation of the surgical specimen (obtained 2 yr after the original resection and 19 mo after radiation therapy) revealed a small number of confluent areas of radionecrosis, extensive reactive gliosis, vascular injury and several small foci of necrosis (Fig. 3). There was also evidence of inflammatory cell reaction, with macrophages, microglia and chronic inflammation. No evidence was found for intrinsic brain neoplasm or recurrent meningioma.

DISCUSSION

FDG-PET is currently the noninvasive gold standard for differentiating recurrent brain tumor from postradiation changes. Although it is difficult to characterize small hypo to eumetabolic lesions by PET in some patients, the presence of intense focal hypermetabolism has always been interpreted as indicating recurrent high-grade tumor.

Recently, there have been several reports of increased FDG accumulation in inflammatory lesion (*9–17*). However, in most of these reports, increased FDG accumulation was detected in peripheral sites and not in the CNS (*9–15*). Since background FDG accumulation is low in most peripheral tissues, even low levels of focal accumulation can be easily visualized. In contrast, the high concentration of FDG in normal brain makes inflammatory accumulation considerably less apparent. In two situations, focal brain abscesses were detected by FDG-PET (*16,17*). However, in both of these cases, the lesion was confined to white matter, and the degree of abnormal localization was much lower than in the present case. Since a frank abscess was not present and the inflammatory changes were of only moderate intensity, the finding of hypermetabolism was even more unusual.

Other imaging procedures that have been used to differentiate recurrent tumor from radiation necrosis are PET with ^{11}C-methionine, ^{201}Tl-SPECT (*6,18–20*) and functional MRI (fMRI). Considering the low incidence of hypermetabolic foci in regions of radiation chances, we do not advocate the use of additional radionuclide procedures. However, fMRI maps of cerebral blood volume can be acquired as minor additions to conventional anatomic MRI. Although there is limited experience with fMRI for differentiating radiation changes from recurrent tumor, preliminary results in our laboratory have been

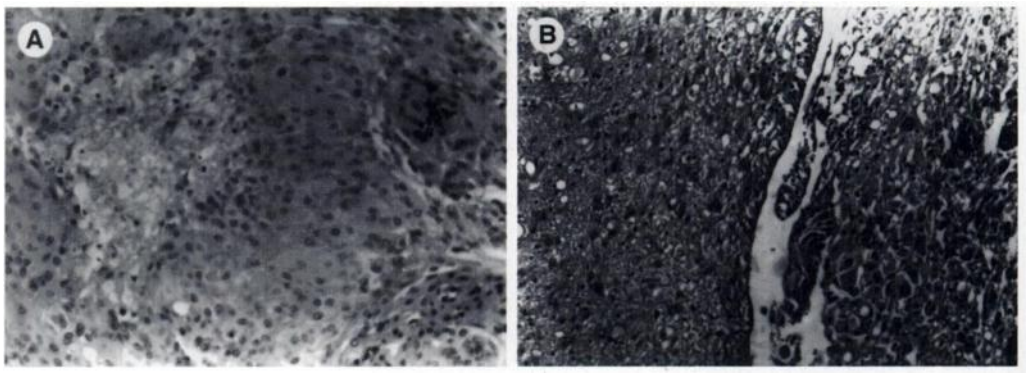

FIGURE 3. (A) Histological section obtained before radiation therapy shows necrosis and atypical meningioma. (B) Histological section obtained after radiation therapy shows necrosis (right), atypical blood vessels (center) and brain tissue with macrophages and reactive astrocytes. Both sections (125x) are stained with hematoxylin and eosin.

promising. Since abnormalities on fMRI and FDG-PET reflect different aspects of tumor metabolism, proliferation of new blood vessels versus elevated glucose metabolism, the techniques are likely to be complementary.

CONCLUSION

This report demonstrates that the finding of intense hypermetabolism by FDG-PET is not pathognomonic for recurrence in patients with brain tumors treated with radiation. However, despite this very infrequent pattern, the procedure remains an extremely important tool for the metabolic evaluation of brain tumors.

REFERENCES

1. Di Chiro G, Oldfield E, Wright DC, et al. Cerebral necrosis after radiotherapy and/or intra-arterial chemotherapy for brain tumors: PET and neuropathologic studies. *Am J Roentgenol* 1988;150:189–197.
2. Valk PE, Budinger TF, Levin VA, Silver P, Gutin PH, Doyle WK. PET of malignant cerebral tumors after interstitial brachytherapy. Demonstration of metabolic activity and correlation with clinical outcome. *J Neurosurg* 1988;69:830–838.
3. Doyle WK, Budinger TF, Valk PE, Levin VA, Gutin PH. Differentiation of cerebral radiation necrosis from tumor recurrence by [^{18}F]FDG and ^{82}Rb PET. *J Comput Assist Tomogr* 1987;11:563–570.
4. Martins AN, Johnston JS, Henry JM, Stoffel TJ, Di Chiro G. Delayed radiation necrosis of the brain. *J Neurosurg* 1977;47:336–345.
5. Dooms GC, Hecht S, Brant-Zawadzki M, Berthiaume Y, Norman D, Newton TH. Brain radiation lesions: MR imaging. *Radiology* 1986;158:149–155.
6. Buchpiguel CA, Alavi JB, Alavi A, Kenyon LC. PET versus SPECT in distinguishing radiation necrosis from tumor recurrence in the brain. *J Nucl Med* 1995;36:159–164.
7. Rota Kops E, Herzog H, Schmid A, Holte S, Feinendegen LE. Performance characteristics of an eight-ring whole-body PET scanner. *J Comput Assist Tomogr* 1990;14:437–445.
8. Alpert NM, Berdichevsky D, Levin Z, Morris ED, Fischman AJ. Improved methods for image registration. *J Neuro Image* 1996;3:10–18.
9. Jones HA, Clark RJ, Rhodes CG, Schofield JB, Krausz T, Haslett C. Positron emission tomography of ^{18}FDG uptake in localized pulmonary inflammation. *Acta Radiol Suppl* 1991;376:148.
10. Yamada S, Kubota K, Kubota R, Ido T, Tamahashi N. High accumulation of fluorine-18-fluorodeoxyglucose in turpentine-induced inflammatory tissue. *J Nucl Med* 1995;36:1301–1306.
11. Larson SM. Cancer or inflammation? A holy grail for nuclear medicine. *J Nucl Med* 1994;35:1653–1655.
12. Palmer WE, Rosenthal DI, Schoenberg OI, et al. Quantification of inflammation in the wrist with gadolinium-enhanced MR imaging and PET with ^{18}F-2-fluoro-2-deoxy-D-glucose. *Radiology* 1995;196:647–655.
13. Jones HA, Clark RJ, Rhodes CG, Schofield JB, Krausz T, Haslett C. In vivo measurement of neutrophil activity in experimental lung inflammation. *Am J Respir Crit Care Med* 1994;149:1635–1639.
14. Tahara T, Ichiya Y, Kuwabara Y, et al. High ^{18}F-fluorodeoxyglucose uptake in abdominal abscesses: a PET study. *J Comput Assist Tomogr* 1989;13:829–831.
15. Fukuda H, Yoshioka S, Watanuki S, et al. Experimental study for cancer diagnosis with ^{18}F-FDG: differential diagnosis of inflammation from malignant tumor. *Kaku Igaku* 1983;20:1189–1192.
16. Sasaki M, Ichiya Y, Kuwabara Y, et al. Ringlike uptake of ^{18}F-FDG in brain abscess: a PET study. *J Comput Assist Tomogr* 1990;14:486–487.
17. Meyer MA, Frey KA, Schwaiger M. Discordance between ^{18}F-fluorodeoxyglucose uptake and contrast enhancement in a brain abscess. *Clin Nucl Med* 1993;18:682–684.
18. Schwartz RB, Carvalho PA, Alexander E, et al. Radiation necrosis versus high-grade recurrent glioma: differentiation by using dual-isotope SPECT with ^{201}TI and ^{99m}Tc-HMPAO. *AJNR* 1991;12:1187–1192.
19. Alexander E, Loeffler JS, Schwartz RB, et al. Thallium-201 technetium-99m-HMPAO SPECT imaging for guiding stereotactic craniotomies in heavily irradiated malignant glioma patients. *Acta Neurochir (Wien)* 1993;122:215–217.
20. Moody EB, Hodes JE, Walsh JW, Thornsberry S. Thallium-avid cerebral radiation necrosis. *Clin Nucl Med* 1994;19:611–613.

Comparative PET Imaging of Experimental Tumors with Bromine-76-Labeled Antibodies, Fluorine-18-Fluorodeoxyglucose and Carbon-11-Methionine

Anna Lövqvist, Anders Sundin, Amilcar Roberto, Håkan Ahlström, Jörgen Carlsson and Hans Lundqvist

Biomedical Radiation Sciences, Departments of Diagnostic Radiology and Pharmaceutical Biosciences, Uppsala University, and Uppsala University PET Centre, Akademiska Sjukhuset, Uppsala, Sweden

The potential of a ^{76}Br-labeled anti-carcinoembryonic antigen monoclonal antibody (MAb), 38S1, as a tumor-imaging agent for PET was investigated in a comparative experimental study with [^{18}F]fluorodeoxyglucose ([^{18}F]FDG) and L-[methyl-^{11}C]methionine ([^{11}C]Met). **Methods:** The three radiotracers were administered to nude rats carrying subcutaneous xenografts or liver metastases from a human colonic carcinoma. Tracer biodistribution was evaluated by PET imaging and radioactivity measurement of dissected tissues and also by whole-body autoradiography for subcutaneous xenografts. **Results:** For PET imaging of subcutaneous tumors, ^{76}Br-38S1 proved superior to the other radiotracers. Tumor-to-tissue ratios were, except for the tumor-to-blood ratio, generally higher for ^{76}Br-labeled MAb than for [^{18}F]FDG and [^{11}C]Met. Liver metastases were imaged with PET using both ^{76}Br-38S1 and [^{18}F]FDG, and the metastases-to-liver ratios of dissected samples were not significantly different for the two radiotracers. **Conclusion:** The tumor-imaging capacity of ^{76}Br-labeled MAb 38S1 was superior to [^{18}F]FDG and [^{11}C]Met in the subcutaneous tumor model, whereas ^{76}Br-38S1 and [^{18}F[FDG were equally successful for the identification of liver metastases.

Received Feb. 28, 1996; revision accepted Sep. 19, 1996.

For correspondence or reprints contact: Anna Lövqvist, MSc, Biomedical Radiation Sciences, Uppsala University, Box 535, S-751 21 Uppsala, Sweden.

Key Words: bromine-76; PET; monoclonal antibodies; fluorine-18-FDG; carbon-11-methionine

J Nucl Med 1997; 38:1029–1035

Several diagnostic problems involving the imaging and characterization of malignant tissues might benefit from the advantages of PET. The quantitative and temporal data obtained with PET can give valuable information about the functional and metabolic status of a lesion. The most commonly used agent for tumor imaging by PET is [^{18}F]fluorodeoxyglucose ([^{18}F]FDG) because the increased metabolic activity of many malignant tumors is reflected by a higher uptake of [^{18}F]FDG than in most normal tissues (*1*). Fluorine-18-FDG-PET has been useful for the detection, staging and treatment monitoring of a variety of malignant diseases (*2*). In the case of colorectal cancer, studies have demonstrated the usefulness of [^{18}F]FDG-PET in imaging of metastatic and recurrent disease (*3–6*). Amino acids as tumor-imaging agents have also proven valuable by taking advantage of an increased membrane transport or protein synthesis rate in the tumor. For instance, L-[methyl-^{11}C]methionine ([^{11}C]Met) has been successfully applied for imaging of tumors in the brain (*7,8*) and in the lung (*9,10*).